Influence of joint modelling on the pushover analysis of a RC frame

Ricardo Costa[*1], Paulo Providência[2a] and Miguel Ferreira[3b]

[1]*Department of Civil Engineering, ISISE, University of Coimbra, Coimbra, Portugal*
[2]*Department of Civil Engineering, INESC Coimbra, University of Coimbra, Coimbra, Portugal*
[3]*CERIS, University of Lisbon, Lisbon, Portugal*

Abstract.   In general, conventional analysis and design of reinforced concrete (RC) frame structures overlook the role of beam-column (RCBC) joints. Nowadays, the rigid joint model is one of the most common for RCBC joints: the joint is assumed to be rigid (unable to deform) and stronger than the adjacent beams and columns (does not fail before them). This model is popular because (i) the application of the capacity design principles excludes the possibility of the joint failing before the adjacent beams and (ii) many believe that the actual behaviour of RCBC joints designed according to the seismic codes produced mainly after the 1980s can be assumed to be nominally rigid. This study investigates the relevance of the deformation of RCBC joints in a standard pushover analysis at several levels: frame, storey, element and cross-section. Accordingly, a RC frame designed according to preliminary versions of EN 1992-1-1 and EN 1998-1 was analysed, considering the nonlinear behaviour of beams and columns by means of a standard sectional fibre model. Two alternative models were used for the RCBC joints: the rigid model and an explicit component based nonlinear model. The effect of RCBC joints modelling was found to be twofold: (i) the flexibility of the joints substantially increases the frame lateral deformation for a given load (30 to 50%), and (ii) in terms of seismic performance, it was found that joint flexibility (ii-1) appears to have a minor effect on the force and displacement corresponding to the performance point (seismic demand assessed at frame level), but (ii-2) has a major influence on the seismic demand when assessed at storey, element and cross-section levels.

Keywords: beam-column joint; reinforced concrete cast-in-situ frames structures; pushover analysis; nonlinear behaviour

1. Introduction

Conventional models of reinforced concrete (RC) framed structures assume that beam-column joints designed according to modern, i.e., post 1980s, seismic technical specifications are fully rigid and stronger than the adjacent beams and columns (Favvata *et al.* 2008). However, several recent studies (Birely *et al.* 2012, Costa 2013, Costa *et al.* 2016b) show that the flexibility of reinforced concrete beam-column (RCBC) joints can have a major contribution to the overall lateral deformation of RC framed structures - this also supports EN 1998-1 (CEN 2004b) requirement that seismic design must consider the joints contribution to the deformation of structures.

However, the unawareness of designers for the relevance of RCBC joints behaviour is not the only reason why their flexibility is usually overlooked in the analysis. Actually, the main reason for this is probably the lack of reliable, clear and objective models for RCBC joints.

Besides, the majority of studies related to RCBC joints deals only with their strength or behaviour and do not assess the influence of RCBC joints on the structure behaviour (Parate and Kumar 2016, Asha and Sundararajan 2014, Shayanfar and Bengar 2016, Wang *et al.* 2015). In fact, there are only a few studies in the literature quantifying the effect of RCBC joints behaviour on the performance of complete RC framed structures and their scope is limited: most of these studies (Calvi *et al.* 2002, Favvata *et al.* 2008, Bayhan *et al.* 2017, Favvata and Karayannis 2014, Sharma *et al.* 2013) (i) are for structures designed before the 1980s, i.e., only for gravity loads, without hoops in the joints and, therefore, having low strength, (ii) typically consider exterior joints, i.e., probably the weakest, (iii) ignore some relevant joint deformation modes or (iv) employ mechanically unsound joint models, most being mere variations of models for beams and columns under bending.

In current structural seismic analysis, the assessment of the seismic performance is based on a single comprehensive limited state and internal forces are usually determined in two steps: a first estimate is based on the assumption of linear elastic behaviour, a reducing behaviour factor being subsequently applied to account for inelastic behaviour - the "equal displacement rule" determines the deformations directly from the structural analysis results (Fardis 2009, Fardis *et al.* 2015). However, a comprehensive limit state for a unique combination of actions is no longer considered rigorous enough and should be replaced by multiple limit states that, if elastic analysis was to be used, would require the definition of multiple behaviour factors. Alternatively, and in order to avoid the complexity inherent to the latter procedure, Performance Based Design methods (e.g.,

---

∗Corresponding author, Ph.D.
 E-mail: rjcosta@dec.uc.pt
[a]Ph.D.
[b]MSc, Ph.D. Student

(SEAOC 1999) and (CEN 2005)) identifying specific performance objectives, besides non-collapse, can be used. The pushover analysis is a feasible alternative to the linear elastic quasi-static analysis and nonlinear dynamic analysis, because, with an acceptable degree of complexity, it explicitly considers the nonlinear behaviour of the structure and the characteristics of the seismic action, without excessive computational effort. Besides, it allows to evaluate the influence of each individual component of the structure on its global behaviour. However, the approximate nature of pushover methods must be stressed out, a nonlineardynamic analysis procedure being advised to increase the reliability of the results.

This study combines a simple nonlinear analysis procedure, the Fictitious Force Method (FFM, Gala *et al.* 2016) with a component based explicit RCBC joint model (Costa *et al.* 2017, Costa 2013), to assess the influence of the beam-column joints modelling in the seismic analysis of a modern RC framed structure through a pushover analysis. Its main conclusion, for the analysed structure, designed according to post 1980s design codes, and for the pushover procedure employed (EN 1998-1), is that the deformability of RCBC joints strongly affects the pushover analysis results.

2. Geometry of the structure

This numerical investigation requires a representative RC framed structure designed to a modern seismic code. The selected structure was designed and tested in the European Laboratory for Structural Assessment (ELSA) of the Joint Research Centre (JRC) - please refer to (Negro *et al.* 1994) and (Arêde 1997) for a comprehensive description of the structure and the tests. Note that the structure was designed according to preliminary versions of EN 1992-1 (CEN, 1984) and EN 1998-1 (CEN 1988) to meet the high ductility class (DCH) requirements, and these standards follow the seismic design philosophy adopted all over the world after the 1980s (e.g., the hierarchy of strength provided by capacity design principles prevents the joints from collapsing before the beams) and thus the structure is representative of post 1980s buildings. This structure was chosen because it is well documented and it was designed by independent and recognised researchers and designers.

This structure with solid slabs has four floors and two bays in each direction, see Fig. 1. The following assumptions were made for design purpose: high seismicity region with a_g=0.3 g, ground type B, importance factor 1 and behaviour factor 5 (Negro *et al.* 1994).

The structure has three frames along each direction, with the interior frames stiffer than the others. They are symmetric along direction x, Fig. 1, but not along the orthogonal direction y, because the spans are different. Our study considers the characteristics of the central frame identified in Fig. 1. The first storey columns are firmly attached to a strong floor, their bottom ends being not allowed to rotate.

The cross-section of the interior and exterior columns is 45 cm×45 cm and 40 cm×40 cm, respectively, the beams
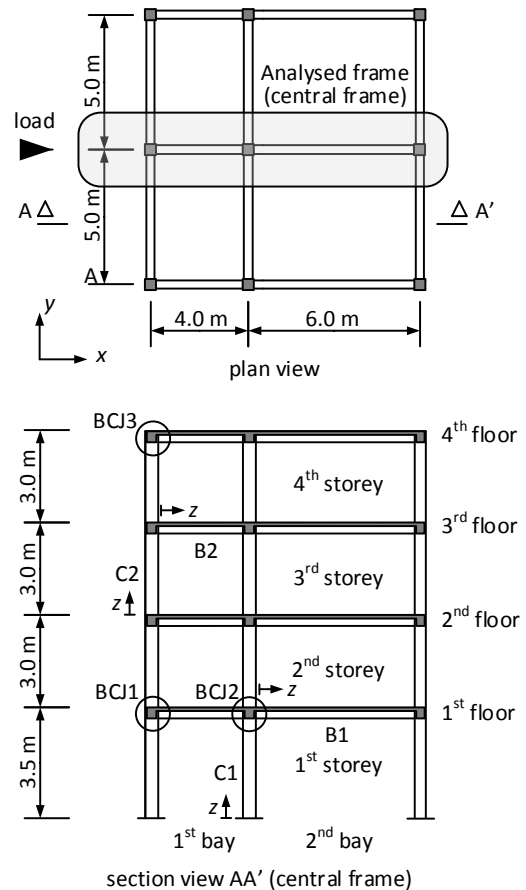

Fig. 1 Framed structure tested at the ELSA laboratory, Ispra (Arêde 1997, Negro *et al.* 1994)

are 30 cm wide and 45 cm high and the slab is 15 cm thick. Rebar detailing of every structural elements is given in Negro *et al.* (1994), Arêde (1997), some examples being shown in Fig. 2. Since no information was found about the transverse reinforcement of the joints (some pictures of the frame after collapse found in the literature make clear that at least three hoops were provided in the joints, e.g., Arêde 1997), we assumed that it is equal to that in the column segments immediately below and above the joint, see Fig. 2.

3. Mechanical properties of structure

3.1 Analysis procedure

The Fictitious Forces Method (FFM) and the FEM software EvalS (Ferreira 2011) were used in the nonlinear analysis of the frame (Gala *et al.* 2016). FFM is an iterative procedure that operates with a constant stiffness in each finite element, and models the material nonlinearity with fictitious loads and the geometric nonlinearity with equivalent loads (Lui 1988). Its main advantages are: (i) simplicity of implementation in linear elastic analysis programs; (ii) similarity of treatment of geometric and material nonlinearities; (iii) being a distributed nonlinear model, it avoids the prior trial and error identification of the regions prone to the development
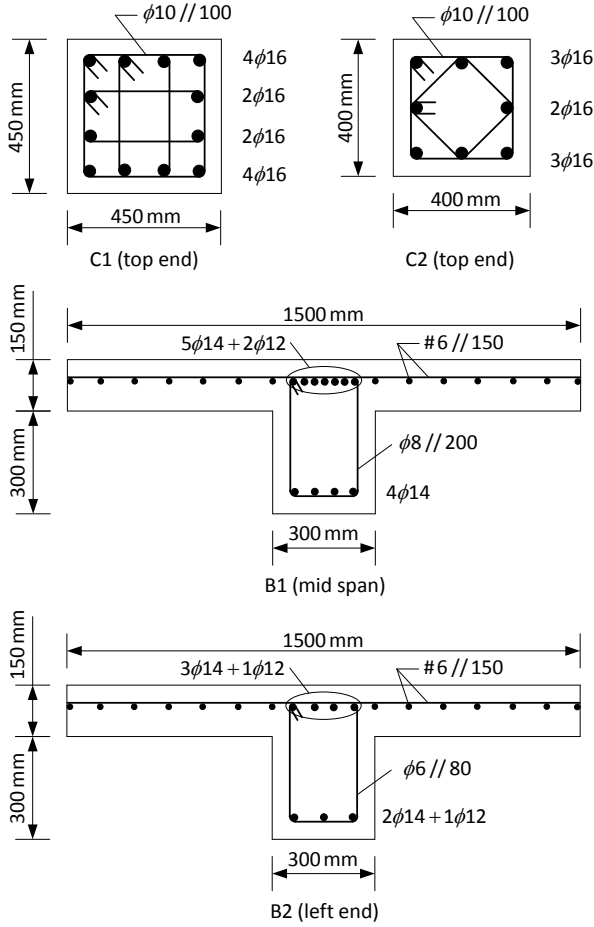
Fig. 2 Cross-sections of columns, beams and slabs (Negro *et al*. 1994, Arêde 1997)

of plastic hinges; (iv) consideration of the coupling between bending and axial behaviour and (v) simplicity of generalization to any type of element, namely the component based RCBC joint model used in this study (Costa *et al*. 2017).

3.2 Mechanical properties of the materials

The concrete compressive strength characteristic value defined in the original design was f_{ck}=25 MPa, for 30 cm high and 15 cm diameter cylinders. For this type of studies EN 1998-1 (CEN 2004b) specifies the use of average values of the materials mechanical properties, for whose determination the analytical relations given in EN 1992-1-1 (CEN 2004a) were employed. For the rebars a bilinear behaviour with yield strength f_y=500 MPa, elasticity modulus E_s=200 GPa, hardening modulus E_{sh}=1 GPa and ultimate strain ε_{su}=10% was considered.

3.3 Beams, columns and slabs

To account for the slabs in the 2D analysis of the central frame, T-beams were considered with effective width of the flanges $b_{ef}=b_w+2(4h_s)$=1500 mm, as suggested by Arêde (1997), where b_w is the beam width and h_s is the thickness of the slab.
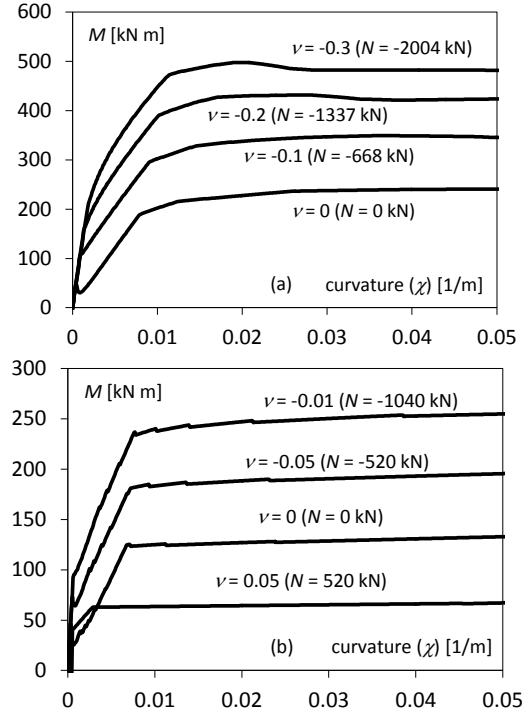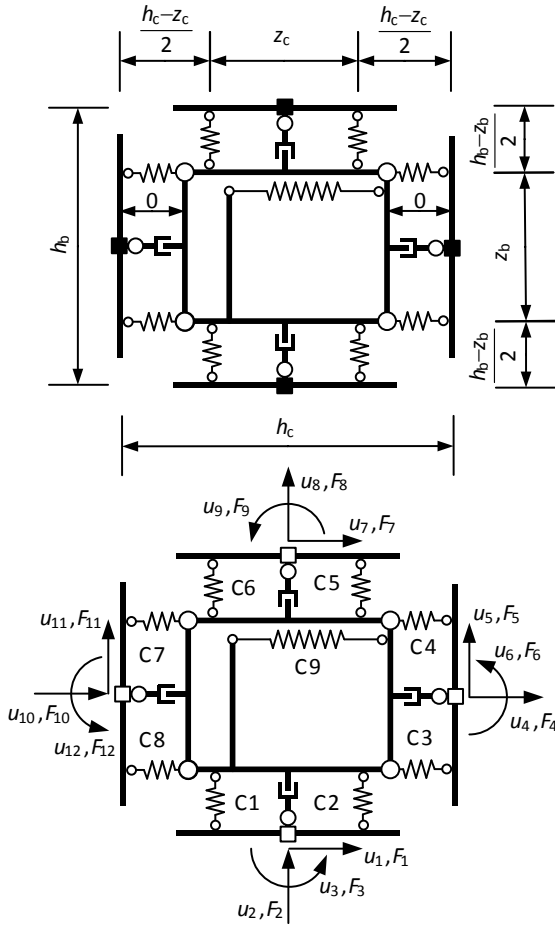

Fig. 3 Cross-section bending moment vs. curvature behaviour: (a) C1 column top end and (b) B1 beam mid span (sagging moments)

The nonlinear cross-sectional behaviour of the T-beams and columns, i.e., the bending moment vs. curvature relation, was computed with a standard fibre model (Gala *et al*. 2016). The beams and columns were discretized longitudinally in at least five elements and their cross-sections in at least thirty fibres.

The nonlinear $\sigma-\varepsilon$ constitutive relationship for concrete in compression developed by Park *et al*. (1982) was employed in order to account for the confinement provided by stirrups and hoops. The concrete inside the core of the elements, i.e., the region bounded by the surface containing the axis of hoops/stirrups, was assumed to be confined and the remaining unconfined. That surface was assumed to be at 25 mm from the face of the beams and columns. In the slabs, following Arêde (1997), the concrete at more than 25 mm from the upper and lower faces was assumed to be confined like that in the core of the beams. Fig. 3 depicts the cross-sectional bending moment vs. curvature relationship ($M-\chi$) for two elements identified in Fig. 1, where $v=N/(A_c f_{cm})$ is the reduced axial force, N is the axial force, A_c is the cross-sectional area and f_{cm} is the uniaxial average compressive strength of concrete.

3.4 Beam-column joints

This study employs a RCBC joint model based on the component method, Fig. 4, developed by Costa (Costa 2013, Costa *et al*. 2017) and proved to be objective (Costa *et al*. 2017). This model required the identification of the joint components ruling the joint behaviour (Biddah and Ghobarah 1999, Altoontash 2004) -joint core in shear, including the effect of joint transverse reinforcement, and anchorages of the adjacent elements in tension and

Fig. 4 RCBC joint model (Costa *et al.* 2017)

Fig. 5 Joint shear behaviour: (a) LaFave and Kim (2011) model, (b) constitutive relation of C9 components

compression-and integrates the corresponding shear component (C9), accounting for joint core shear deformation, and eight anchorage components (C1-8), two for each adjacent beam and column, accounting for their tension and compression anchorages. The model has twelve degrees of freedom, Fig. 4, and is fully compatible with the beam and column elements commonly employed in 2D analysis. It can be used for every type of RCBC joint, i.e., exterior, interior, and corner, if suitable constitutive relations are determined for their components.

The constitutive relation of the shear component (C9) is based on the model developed by LaFave and Kim (2011) for the cyclic shear envelope of RCBC joints. It was defined in terms of the τ_{jh}–γ relation, where γ is the joint global shear strain and τ_{jh} is an average shear stress at joint mid-height and accounts for the following parameters: (i) out-of-plane geometry (presence of transverse beams), (ii) joint eccentricity between the beam and column axes, (iii) joint transverse reinforcement volume and yield strength, (iv) beam longitudinal reinforcement area and yield strength, (v) in-plane geometry of the joint (interior, exterior or knee), and (vi) concrete compressive strength.

The τ_{jh}–γ relation, see Fig. 5, is a polygonal chain defined by the origin and four other points: (A) joint's core cracking; (B) yielding of joint ties or beams longitudinal rebars; (C) ultimate shear strength; and (D) end. Point D merely defines the last, softening, branch.
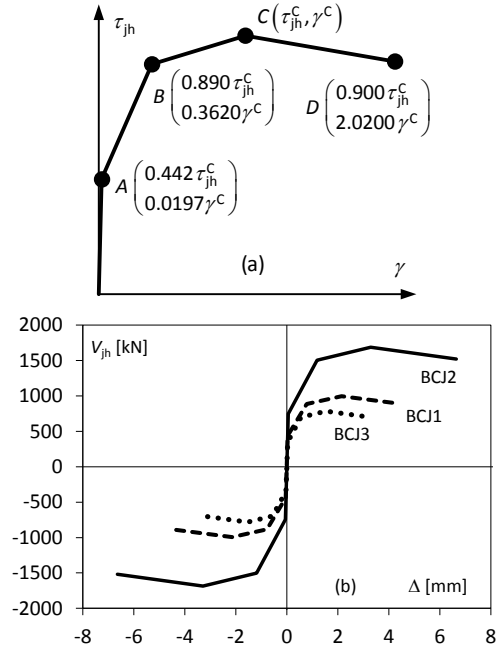
The behaviour of the C9 component is described by the V_{hj}–Δ relation, where $\Delta = \gamma z_b$ and V_{jh} is the horizontal shear force at mid-height of the joint, given by $V_{jh} = \tau_{jh} h_c b_{j,ef}$, h_c being the column cross section height and $b_{j,ef}$ the effective joint width. Fig. 5(b) shows the behaviour of the shear components of the joints identified in Fig. 1: BCJ1 (exterior), BCJ2 (interior) and BCJ3 (corner).

The behaviour of the anchorage components (C1-8) is based on the anchorage models developed by Costa *et al.* (Costa 2013, Costa *et al.* 2016a), where the straight and bent anchorages are decomposed in a number of elements or *cells*. The models for these cells are also based on the component method: (i) straight anchorage cells have two parallel components-the bond component and the rebar component-, and (ii) bent anchorage cells have three components-the bond, the rebar and the bearing concrete components.

The bond component uses the bond stress-slip constitutive relation from MC90 (MC90 1990) for "confined concrete and other bond conditions". The bearing concrete component uses the linear model developed by Soroushian *et al.* (1987). The rebar component uses the bi-linear constitutive relation used for beams and columns. However, because the anchorage lengths are large enough to prevent pull-out failure, they only fail when the tensile strength of the rebars is reached, i.e., when the bending strength of the beam or column end cross-section is reached. To enforce this simultaneity in the numerical model, which could otherwise be violated because of the simplified computation of the internal arms of beams and columns in the joint element, the strength of the anchorages was artificially increased by assigning to the ultimate strain of the rebars in the anchorage components twice the value of the longitudinal rebars in beams and columns, while keeping $E_{sh} = 1$ GPa.
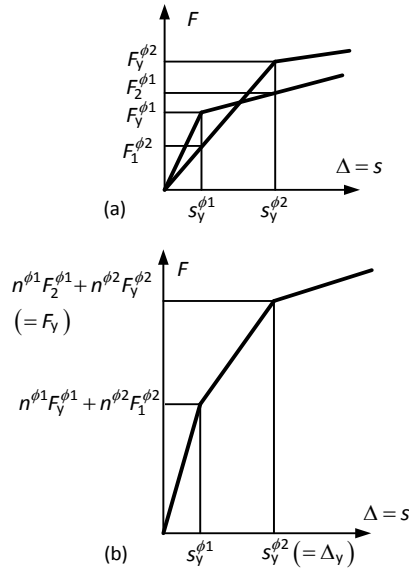
Fig. 6 Simplified behaviour of a tension anchorage with rebars of different sizes: anchorage with (a) one rebar with diameter $\phi1$ and one rebar with diameter $\phi2 > \phi1$, (b) $n^{\phi1} + n^{\phi2}$ rebars with diameter $\phi1$ and $\phi2$, respectively
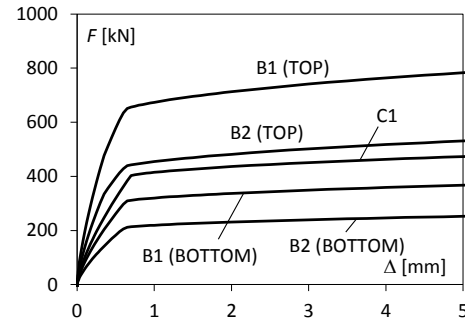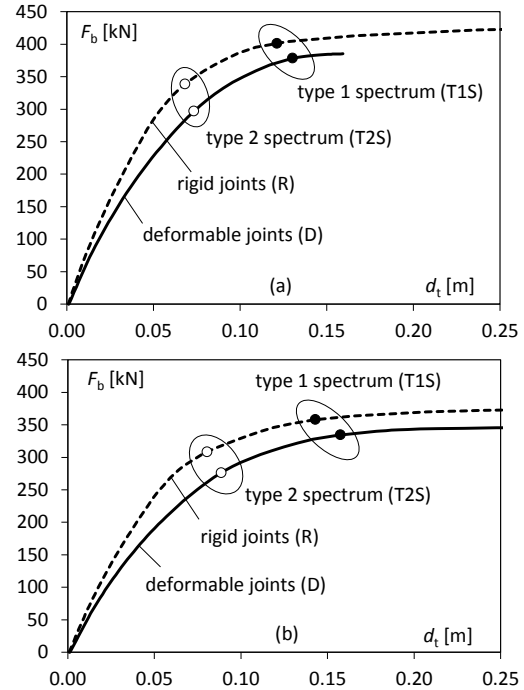

Fig. 7 Behaviour of the anchorage components in tension

Fig. 8 Capacity curves of the frame for the uniform (top) and modal (bottom) lateral forces distributions

In the anchorage components, the longitudinal rebars in the flange of the T-beam were assumed to be anchored in the RCBC joint. To compute the overall behaviour of each tension anchorage in a given joint, note that even though all rebars are placed at the same depth, their strain will vary with the diameter, because the slip at the BC joint interface (s) is a function of the diameter, so that they will not yield simultaneously. This is illustrated for a bilinear law, to simplify the explanation, in Fig. 6 by means of the distinct behaviour of two bars, 1 and 2, with $\phi2 > \phi1$. When bar 1 yields the axial force is $F_y^{\phi1}$ in bar 1 and $F_1^{\phi2}$ in bar 2. Similarly, when bar 2 yields the axial force is $F_y^{\phi2}$ in bar 2 and $F_2^{\phi1}$ in bar 1. The figure also depicts the combined behaviour of $n^{\phi1}$ bars of type 1 and $n^{\phi2}$ bars of type 2. To compute the behaviour of the anchorage component in compression the procedure suggested by Lowes *et al.* (2004) was used.

The springs representing the anchorages components are characterized by $F{-}\Delta$ relations, where F is the tension or compression resultant transmitted by the beam or column to the joint and Δ is the slip of the anchorage at the joint's interface with the column/beam (tension anchorages) or the anchorage region shortening (compression anchorages). Fig. 7 represents the behaviour of the anchorage components of some elements identified in Fig. 1.

4. Pushover analysis

4.1 Preliminary considerations

The assessment of earthquake effects must account for the simultaneous action of gravity loads. For this purpose, following Arêde (1997), uniformly distributed loads on the

beams, of 35 kN/m in the top floor and 34 kN/m in the remaining floors, were considered. Furthermore, part of the mass in each floor was assumed to be associated to the frame analysed.

To simulate the inertia forces due to the seismic action EN 1998-1 proposes two alternative vertical distributions of lateral forces acting on the floors: the so called uniform pattern (*U*), which is proportional to the floor masses, and the modal pattern (*M*), which is proportional to the floor masses and to their displacement in the fundamental mode shape. These horizontal loads were distributed uniformly along the beams in order to get an accurate axial force distribution in them, a crucial requisite because of the nonlinear coupling between bending and axial behaviour (Gala *et al.* 2016).

4.2 Frame level analysis

4.2.1 Capacity curves

For a given structure and lateral forces distribution, the capacity curve is the $F_b(d_t)$ function, where F_b is the base
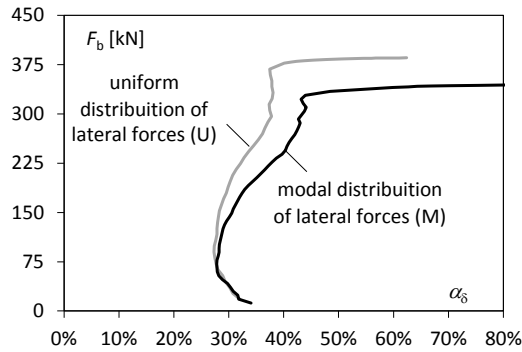
Fig. 9 Influence of the lateral forces distribution shape and magnitude on the contribution of the RCBC joint flexibility to the frame lateral displacement
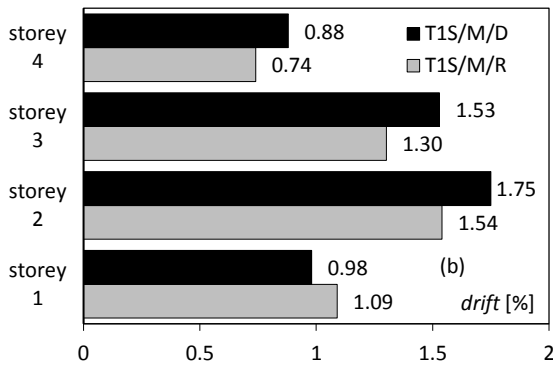

Fig. 10 Pushover analysis for the Type 1 response spectrum for a modal distribution of lateral loads: (a) lateral displacement of the floors and (b) interstorey drift

shear force and d_t the displacement at roof level (control node), determined for fixed gravity loads and increasing amplitude of the lateral forces distribution. Fig. 8 depicts the determined capacity curves for two frame models: one with rigid (*R*) and the other with deformable (*D*) RCBC joint models. Since a load control procedure was used, the interruption of the capacity curves in Fig. 8 corresponds to a limit point, not to collapse. In the present investigation, the only purpose of these capacity curves is the evaluation of the influence of the RCBC joint models in terms of relative performance, e.g., the variation of target displacements, which occur before the limit point.

4.2.2 Target displacements

The target displacements were computed according to the procedure proposed in Annex B of EN 1998-1 for 5% viscous damping. They are shown in Fig. 8 for both lateral load distributions and EN 1998-1 Type 1 (T1S) and Type 2 (T2S) horizontal elastic response spectra. Table 1 shows the determined target displacement and the corresponding base shear force.

For a given value of the base shear force, the effect of joint deformability is given by the ratio

$$\alpha_\delta = \frac{d_t^D - d_t^R}{d_t^R} \qquad (1)$$

represented in Fig. 9. This figure shows that, for a given

Table 1 Determined values of target displacement

response spectrum	Type 1 (T1S)			Type 2 (T2S)		
joint model	rigid (R)	def. (D)	(D-R)/R [%]	rigid (R)	def. (D)	(D-R)/R [%]
	uniform load pattern (U)					
d_t [m]	0.121	0.130	7.4	0.068	0.073	7.3
F_b [kN]	401.2	378.2	-5.7	338.5	296.8	-12.3

load, joint deformability causes a 30% to 50% increase of the frame lateral deformation.

Fig. 8 and Table 1 show that even though joint deformability may cause a very large increase of the structure lateral displacements for a given load level, it has a smaller influence in terms of the target displacement: the joint deformability is responsible for a 30 to 50% increase in the frame lateral deformations, for a given load level (Fig. 9) and of only about 10% increase of the displacement in the frame roof for the computed target displacements (Fig. 8 and Table 1).

4.3 Storey level analysis - interstorey drifts

The cases with larger target displacement, identified by shaded cells in Table 1, correspond to the Type 1 spectrum (T1S) and a modal distribution of lateral forces (M). For the sake of brevity, the effect of the joints deformability is examined in terms of local quantities only for these cases. Fig. 10 represents the interstorey drift, corresponding to the target displacements values, for rigid (T1S/M/R) and deformable (T1S/M/D) joint behaviour. It can be seen that the influence of the RCBC joint deformability on the interstorey drift is larger than on the value of the target displacements. Actually, when the RCBC joints deformability is accounted for in the analysis, the interstorey drift increases more than the target displacements in every storey except the first: −10% in the 1st storey (decrease), and 14%, 18% and 19% in the 2nd, 3rd and 4th storeys, respectively (increase).

The interstorey drift gives a measure of damage in structural and non-structural elements (CEN 2004b), so that this damage may be underestimated if the RCBC joints deformation is not accounted for.

According to EN 1998-1, second order effects may be ignored in ultimate limit state analysis if the interstorey drift sensitivity coefficient θ, which measures the sensitivity of the structure to these effects, satisfies the following condition

$$\theta = \frac{P_{tot}\, d_r}{V_{tot} h} \leq 0.10 \qquad (2)$$

where P_{tot} is the total gravity load at and above the storey considered in the seismic design situation, d_r is the design interstorey drift, given by the difference of the average lateral displacements at the top and bottom of the storey under consideration, V_{tot} is the total seismic storey shear and h is the storey height. The computed θ values are listed in Table 2, showing, as expected, that in the present case (i) because the gravity loads are low and the columns are

Table 2 Sensitivity coefficient corresponding to the target displacements T1S/M/R (θ_R) and T1S/M/D (θ_D)

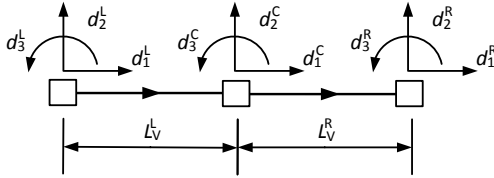| storey	θ_R [%]	θ_D [%]	$(\theta_D - \theta_R)/\theta_R$ [%]
1	3.8	3.6	-5
2	4.3	5.3	23
3	3.2	4.0	25
4	1.7	2.1	24

Fig. 11 Nodal coordinate system for beam and column elements

bulky, second order effects are not relevant, and (ii) the deformability of RCBC joints increases substantially the sensitivity of the structure to second order effects in some storeys (23, 25 and 24% in the 2nd, 3rd and 4th storeys, respectively).

The relative increase of θ in the three top storeys due to joint deformability more than doubles the relative increase for the corresponding target displacements (approximately 10%, see Table 1) and is also higher than the relative increase of the interstorey drift. This is because in these storeys the target displacement T1S/M/D corresponds simultaneously to greater storeys drifts and lower storey shears than for the T1S/M/R case, i.e., $d_r^D > d_r^R$ and $V_r^D < V_r^R$.

4.4 Element level analysis - shear span chord rotation

According to EN 1998-3, the shear span chord rotation of beams and columns gives a measure of their deformation. To compute this rotation, the shear span of each element was assumed to be half of its clear length, $L_V = L/2$ (Fardis 2009). Thus, if in each element two end nodes, L and R, and a mid-span node, C, are considered, the left and right chord rotations are given by, see Fig. 11

$$\theta^L = \arctan\left(\frac{d_2^C - d_2^L}{L/2}\right) - d_3^L \quad \text{and}$$

$$\theta^R = \arctan\left(\frac{d_2^R - d_2^C}{L/2}\right) - d_3^R \tag{3}$$

where d_3^L and d_3^R are the end nodes rotations and d_2^L, d_2^C and d_2^R are the node deflections.

Fig. 12 gives a graphical representation of the chord rotations demand corresponding to the target displacements T1S/M/R and T1S/M/D and Fig. 13 their values. These figures reveal that the deformability of the RCBC joints substantially reduces the deformation demand in beams and columns. Hence, ignoring the joint deformability in the analysis overestimates the damage in beams and columns
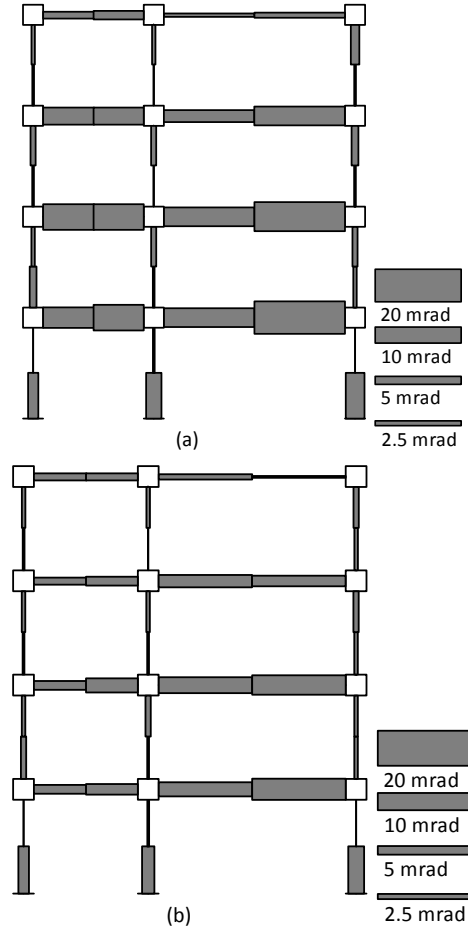

Fig. 12 Chord rotations of beams and columns corresponding to the target displacement for (a) rigid (T1S/M/R) and (b) deformable (T1S/M/D) joints

and underestimates the deformation demand in RCBC joints, leading to a poor assessment of the seismic performance of the structure.

4.5 Cross sectional analysis - internal forces and local deformations

In the assessment of the seismic performance of structures by a displacement based procedure (SEAOC 1999) and (Fardis 2009), like the one used herein, the internal forces are required for assessing, not the ductile mechanisms, but only the fragile mechanisms, e.g., the shear mechanism in beams and columns and RCBC joints.

Fig. 14 represents the bending moment (M) and axial force (N) along the beams and columns labelled in Fig. 1, corresponding to the target displacements T1S/M/R and T1S/M/D. It clearly shows that the bending moment fields in elements B1, B2, C1 and C2 are not very sensitive to joint deformability. In contrast, the axial force fields seem to be strongly affected by joint deformability. However, a much more meaningful parameter is the reduced axial force v: its absolute variation with the joint deformability is less than 0.005, which is irrelevant for the pushover analysis. Figs. 15 and 16 show the bending moment and axial force at the end of beams and columns for the target displacements
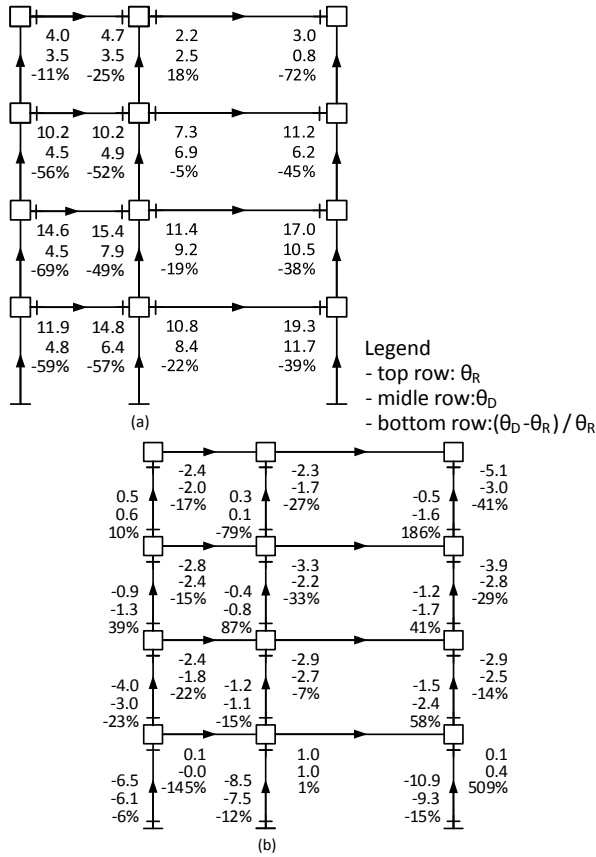
Fig. 13 Chord rotations (mrad) of beams and columns corresponding to the target displacement with rigid (θ_R; T1S/M/R) and deformable joints (θ_D; T1S/M/D): (a) beams, (b) columns
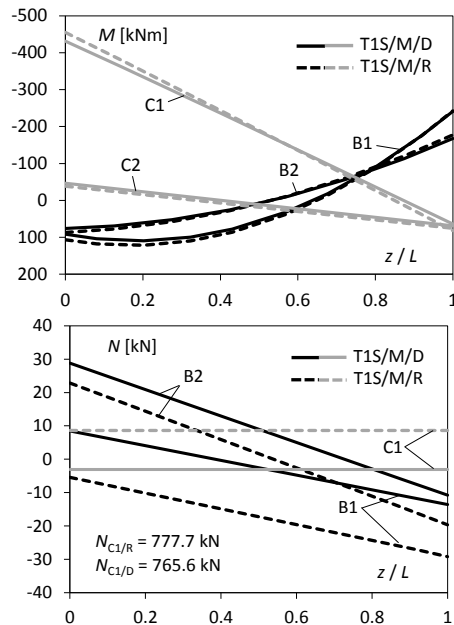

Fig. 14 Bending moment and axial force fields in some beams and columns
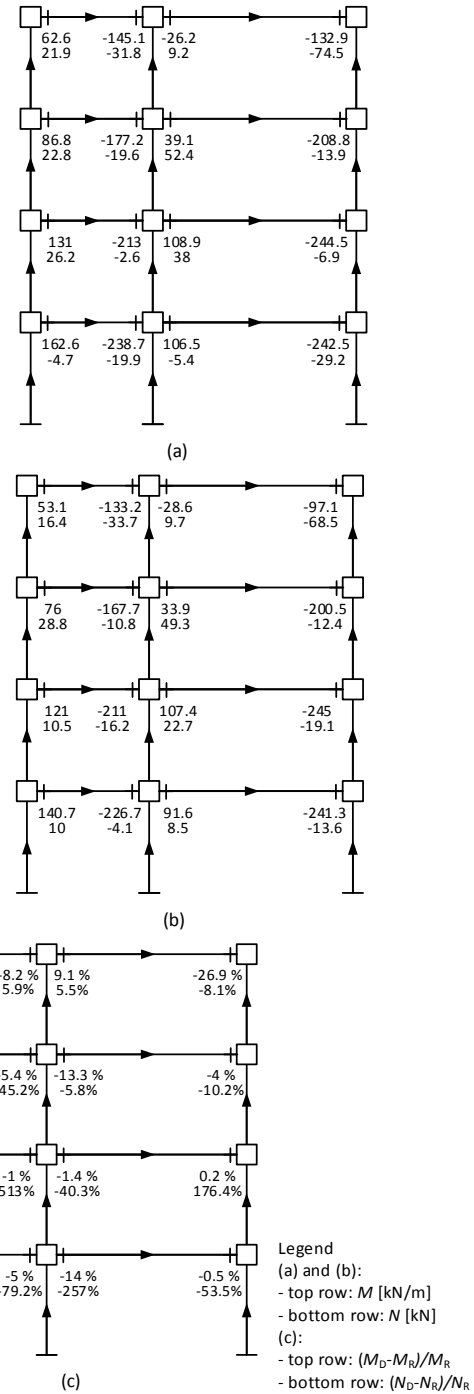

Fig. 15 Bending moment and axial force in beams corresponding to the target displacement for (a) rigid (T1S/M/R) and (b) deformable (T1S/M/D) joints. Relative variation in (c)

T1S/M/R and T1S/M/D, revealing that in some cases the joint flexibility may cause substantial changes in bending moment distributions. The bending moment distributions

due to the flexibility of RCBC joints is smaller than the changes of the chord rotations see Figs. 12 and 13 mainly because (i) the similar base shear force values (Table 1) corresponding to the target displacements T1S/M/D and T1S/M/R, and also (ii) the lateral displacements being larger for the target displacement T1S/M/D case than for the T1S/M/R case, partially compensating, by means of the second-order effects, the different magnitude of the applied equivalent horizontal seismic forces.
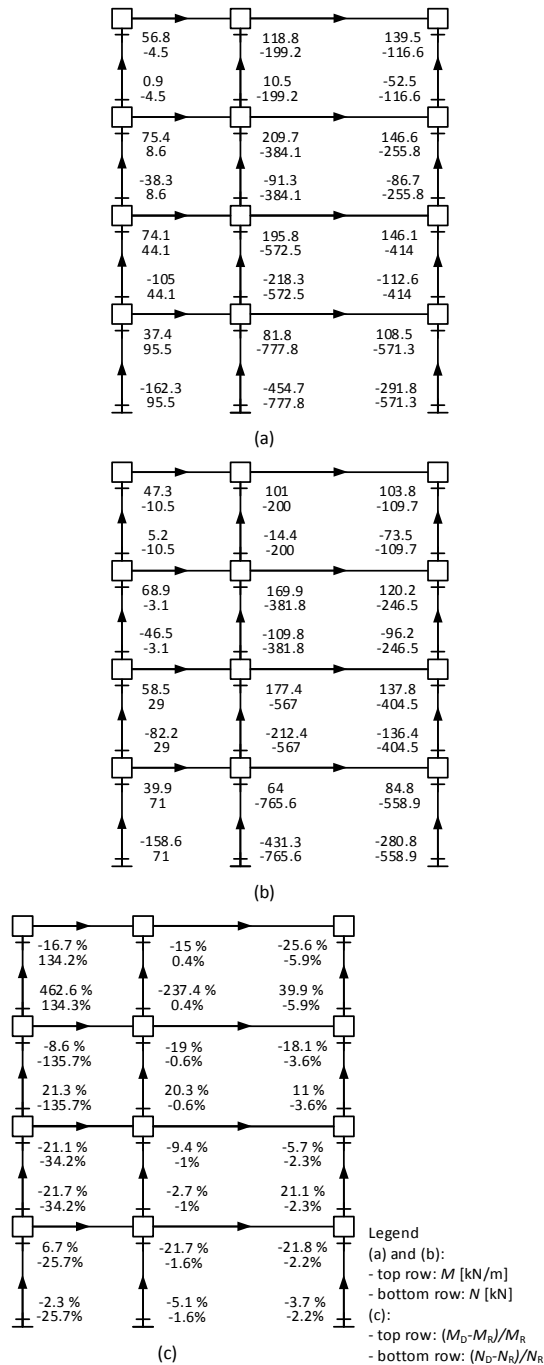
Fig. 16 Bending moment and axial force in columns corresponding to the target displacement with (a) rigid (T1S/M/R) and (b) deformable (T1S/M/D) joints. Relative variation in (c)

Fig. 17 Curvature field in beams and columns
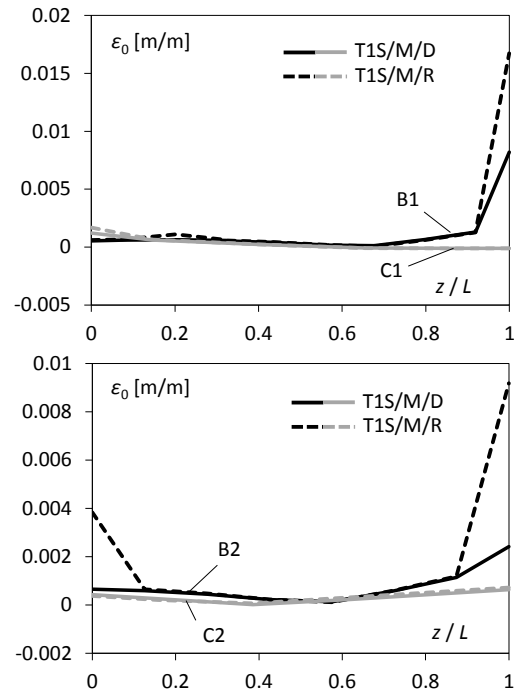
Fig. 18 Axial deformation field in beams and columns

For the beams and columns labelled in Fig. 1, the curvature (χ) and axial elongation (ε_0) for the target displacements are represented in Figs. 17 and 18, showing that they are substantially affected by the joints deformability in the regions where the plastic deformations are larger, i.e., near the ends of the beams and columns, see also Figs. 19 and Fig. 20. These figures also show the ratio χ/χ_y, graphically depicted in Fig. 21, χ_y being the curvature corresponding to the yielding of the longitudinal rebars for the same axial load level. The figures reveal that the
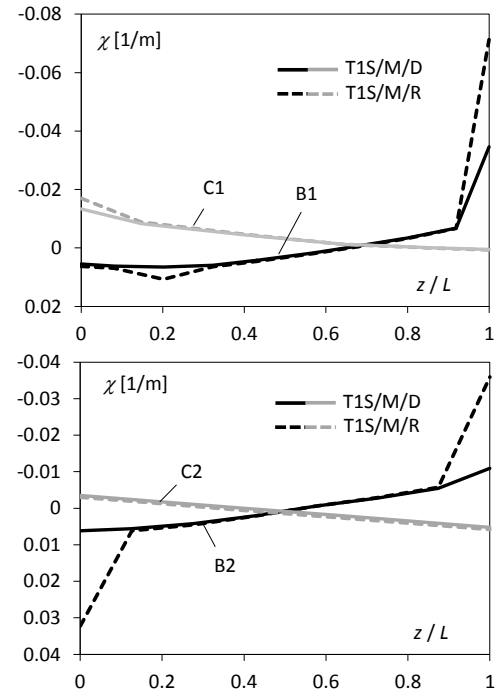
deformability of the RCBC joints substantially reduces the deformation demand in beams and columns-e.g., in the exterior ends of the second floor beams χ/χ_y are reduced from 8.05 and 6.77 to 0.99 and 3.36 when the RCBC joint flexibility is considered. Hence, it can be concluded, as from the shear span chord rotation, that ignoring the joint deformability in the analysis overestimates the damage in beams and columns, underestimates the deformation demand in the joints and leads to a poor assessment of the seismic performance of the structure.
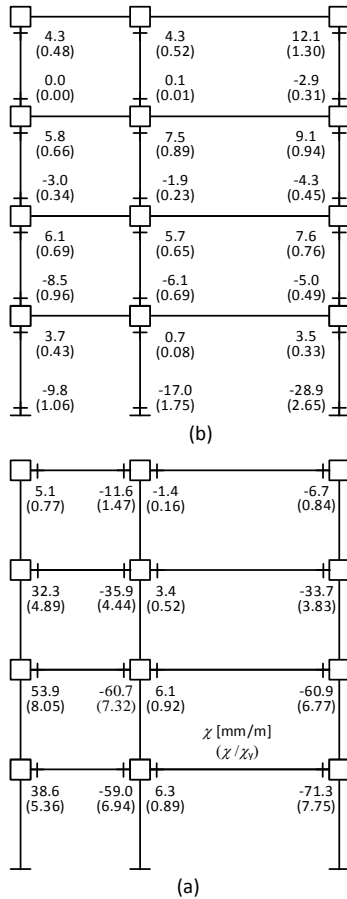
Fig. 20 Continued

Fig. 19 Curvature at (a) beam and (b) column ends corresponding to the target displacement with rigid joints (T1S/M/R)
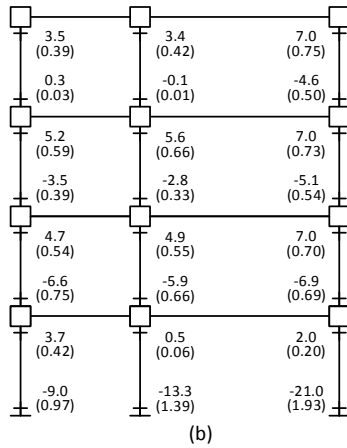

Fig. 20 Curvature at (a) beam and (b) column ends corresponding to the target displacement with deformable joints (T1S/M/D)

4.6 Deformation of beam-column joints

Fig. 22 represents the ratio Δ/Δ_y for each component of the RCBC joint model, where Δ is the component deformation corresponding to the target displacement T1S/M/D and Δ_y is that corresponding to yielding, for components C1 to C8, and to the ultimate shear strength,
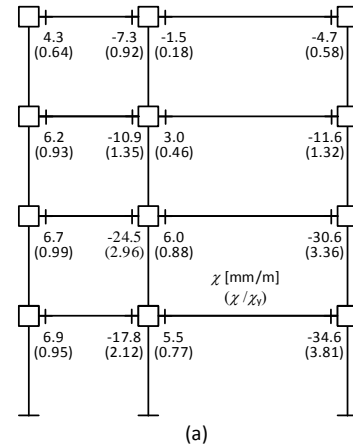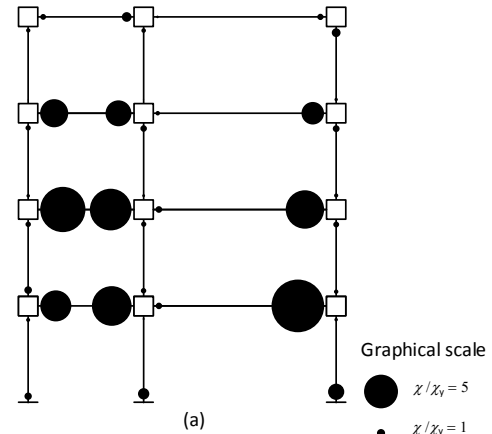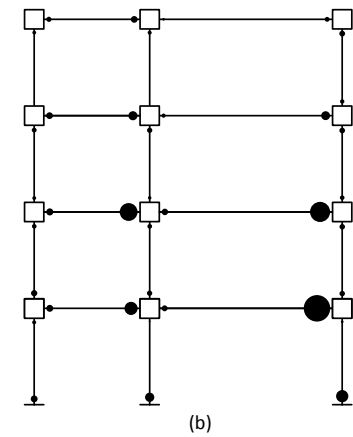

Fig. 21 Graphical representation of the ratio χ/χ_y in beams and columns corresponding to the target displacement with (a) rigid (T1S/M/R) and (b) deformable joints (T1S/M/D)

i.e., Δ_C, for component C9. This figure shows that the joint shear deformation (C9) is small when compared with the deformation of the other joint components (C1-8) - this is probably due to the cross-section being larger for columns than beams and to the high transverse reinforcement ratio in the RCBC joints. However, a substantial contribution of the joint shear deformation is expected in structures with slender columns, e.g., with comparable cross-sections of beams and columns, and larger longitudinal reinforcement ratios in these elements (Costa 2013, Costa *et al.* 2017).
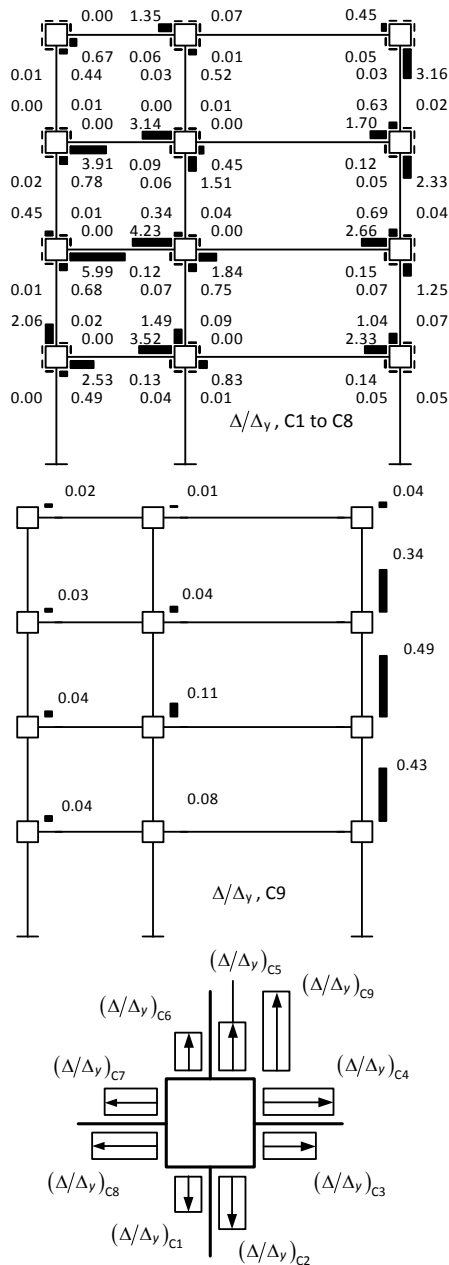
Fig. 22 Deformations on the joint components corresponding to the target displacement with deformable joints (T1S/M/D)

These results are in close agreement with the visual observations of the crack pattern in the tested frame: instead of the cracks typical of the flexural hinges in beams and columns, major cracks were observed in the interface between the beams and the columns (in external joints also inclined cracks were observed in the joint core) suggesting that the yielding of rebars took place locally and the steel-concrete bond inside the joint core might have been seriously damaged, leading to substantial bar-slippage inside the joints (Negro 1997, Arêde 1997).

5. Conclusions

A pushover analysis of a modern RC frame according to EN 1998-1 shows that the deformability of RCBC joints (i) is the cause for a substantial part of the frame lateral displacement, for a given load level (from 30 to 50%), and (ii) has small impact on the target displacement. However, the analysis of the local deformations (interstorey drift, shear span chord rotations and curvature of beams and columns) shows that joint deformability has a strong influence on the results of the pushover analysis. It was found that ignoring the deformability of RCBC joints causes (i) an underestimation of the maximum drift and of the second-order effects, (ii) an overestimation of the deformations in beams and columns, and, consequently, (iii) wrong estimates of the expectable damage in these elements. It is therefore clear that, even in RC framed structures designed according to modern seismic technical specifications, the RCBC joints should not be modelled as rigid for structural analysis purposes. The results presented in this paper are limited to the chosen structure and pushover analysis procedure.

References

Altoontash, A. (2004), "Simulation and damage models for performance assessment of reinforced concrete beam-column joints", Stanford University.
Arêde, A. (1997), "Seismic assessment of reinforced cncrete frame structures with a new flexibility based element", University of Porto.
Asha, P. and Sundararajan, R. (2014), "Experimental and numerical studies on seismic behaviour of exterior beam-column joints", *Comput. Concrete*, **13**(2), 221-234.
Bayhan, B., Özdemir, G. and Gülkan, P. (2017), "Impact of joint modeling approach on performance estimates of older-type rc buildings", *Earthq. Spectra*, **33**(3), 1101-1123.
Biddah, A. and Ghobarah, A. (1999), "Modelling of shear deformation and bond slip in reinforced concrete joints", *Struct. Eng. Mech.*, **7**(4), 413-432.

Figs. 12 and 22 show that, when the RCBC joints are assumed as rigid, part of the deformation demand in beams and columns actually take place in the joints, even though the ends of beams/columns with larger θ^L, θ^R and χ/χ_y do not perfectly match the joint components with larger Δ/Δ_y, which means that this redistribution is not merely local.

The differences found for the values of θ^L, θ^R and χ/χ_y in the context of seismic design based on a nonlinear static analysis is particularly relevant because the structural performance can be directly evaluated in terms of these parameters. This means that wrong estimates of these quantities will inevitably lead to wrong conclusions about the seismic performance. This is particularly relevant in the assessment of existing structures.

Birely, A.C., Lowes, L.N. and Lehman, D.E. (2012), "A model for the practical nonlinear analysis of reinforced-concrete frames including joint flexibility", *Eng. Struct.*, **34**, 455-465.

Calvi, G., Magenes, G. and Pampanin, S. (2002), "Relevance of beam-column joint damage and collapse in RC frame assessment", *J. Earthq. Eng.*, **6**, 75-100.

CEN (1984), "Eurocode 2, Common unified rules for concrete structures", Commission of the European Communities.

CEN. (1988), "Eurocode 8, Structures in seismic regions-Design-Part 1, General and Bulding", Commission of the European Communities.

CEN (2004a), "EN 1992-1-1, Eurocode 2: Design of Concrete Structures-Part1-1: General Rules and Rules for Buildings", European Committee for Standardisation, Brussels.

CEN (2004b), "EN 1998-1, Eurocode 8: Design of structures for earthquake resistance-Part 1: General rules, seismic actions and rules for buildings", European Committee for Standardisation, Brussels.

CEN (2005), "EN 1998-3, Eurocode 8: Design of structures for earthquake resistance-Part 3: Assessment and retrofitting of buildings", European Committee for Standardisation, Brussels.

Costa, R. (2013), "Beam-column joints modelling for the analysis of reinforced concrete plane frames", University of Coimbra, Portugal. (in Portuguese)

Costa, R., Providência, P. and Dias, A. (2016a), "Anchorage models for reinforced concrete beam-column joints under quasi-static loading", *ACI Struct. J.*, **113**(3), 503-514.

Costa, R., Providência, P. and Dias, A. (2017), "Component based reinforced concrete beam-column joint model", *Struct. Concrete*, **18**(1), 164-176.

Costa, R., Providência, P. and Gomes, F. (2016b), "On the need for classification criteria of cast in situ rc beam-column joints according to their stiffness", *Mater. Struct.*, **49**(4), 1299-1317.

Fardis, M.N. (2009), *Seismic Design, Assessment and Retrofitting of Concrete Buildings Based on EN-Eurocode 8*, Springer.

Fardis, M.N., Carvalho, E.C., Fajfar, P. and Pecker, A. (2015), *Seismic Design of Concrete Buildings to Eurocode 8*, CRC Press.

Favvata, M.J., Izzuddin, B.A. and Karayannis, C.G. (2008), "Modelling exterior beam-column joints for seismic analysis of rc frame structures", *Earthq. Eng. Struct. Dyn.*, **37**(13), 1527-1548.

Favvata, M.J. and Karayannis, C.G. (2014), "Influence of pinching effect of exterior joints on the seismic behavior of RC frames", *Earthq. Struct.*, **6**(1), 89-110.

Ferreira, M. (2011), "EvalS 2.2 (http://evalssoftware.blogspot.pt/)", Leiria.

Gala, P., Costa, R., Ferreira, M., Providência, P. and Dias, A. (2016), "The fictitious forces method and its application to the nonlinear analysis of rc skeletal structures", *ASCE J. Struct. Eng.*, **142**(11), 04016107.

LaFave, J.M. and Kim, J.H. (2011), "Joint shear behavior prediction for rc beam-column connections", *Int. J. Concrete Struct. Mater.*, **5**(1), 57-64.

Lowes, L., Mitra, N. and Altoontash, A. (2004), "A beam-column joint model for simulating the earthquake response of reinforced concrete frames", PEER, University of California.

Lui, E.M. (1988), "A practical p-delta analysis method for type FR and PR frames", *Eng. J. AISC*, **25**(3), 85-98.

MC90 (1990), "ceb-fip model code 1990-design code", Comite Euro-International du Beton-The International Federation for Structural Concrete, Thomas Telford, London.

Negro, P. (1997), "Experimental assessment of the global cyclic damage of framed r/c structures", *J. Earthq. Eng.*, **1**(3), 543-562.

Negro, P., Verzeletti, G., Magonette, G.E. and Pinto, A.V. (1994), "Tests on a four-storey full-scale r/c frame designed according to Eurocodes 8 e 2: preliminary report", ELSA Laboratory, Luxembourg.

Parate, K. and Kumar, R. (2016), "Investigation of shear strength models for exterior RC beam-column joint", *Struct. Eng. Mech.*, **58**(3), 475-514.

Park, R., Priestley, M.J.N. and Gill, W.D. (1982), "Ductility of squared-confined concrete columns", *J. Struct. Div.*, ASCE, **108**(4), 929-950.

SEAOC (1999), "Recommended lateral force requirements and commentary", Structural Engineers Association of California, Sacramento.

Sharma, A., Reddy, G.R., Vaze, K.K. and Eligehausen, R. (2013), "Pushover experiment and analysis of a full scale non-seismically detailed RC structure", *Eng. Struct.*, **46**, 218-233.

Shayanfar, J. and Bengar, H.A. (2016), "Numerical model to simulate shear behaviour of RC joints and columns", *Comput. Concrete*, **18**(4), 877-901.

Soroushian, P., Obaseki, K. and Rojas, M.C. (1987), "Bearing strength and stiffness of concrete under reinforcing bars", *ACI Mater. J.*, **84**(3), 179-184.

Wang, L., Fan, G. and Song, Y. (2015), "Effect of loading velocity on the seismic behavior of RC joints", *Earthq. Struct.*, **8**(3), 665-679.

CC